

Femtosecond Transient Absorption Anisotropy Study on $[\text{Ru}(\text{bpy})_3]^{2+}$ and $[\text{Ru}(\text{bpy})(\text{py})_4]^{2+}$. Ultrafast Interligand Randomization of the MLCT State

Staffan Wallin,[†] Jan Davidsson,[†] Judit Modin,[‡] and Leif Hammarström^{*,†}

Department of Physical Chemistry, Uppsala University, Box 579, SE-75123 Uppsala, Sweden, and
Department of Chemistry, Organic Chemistry, Uppsala University, Box 599, SE-75124 Uppsala, Sweden

Received: February 22, 2005; In Final Form: March 21, 2005

It is known that the relaxed excited state of $[\text{Ru}(\text{bpy})_3]^{2+}$ is best described as a metal to ligand charge transfer (MLCT) state having one formally reduced bipyridine and two neutral. Previous reports have suggested [Malone, R. et al. *J. Chem. Phys.* **1991**, 95, 8970] that the electron “hops” from ligand to ligand in the MLCT state with a time constant of about 50 ps in acetonitrile. However, we have done transient absorption anisotropy measurements indicating that already after one picosecond the molecule has no memory of which bipyridine was initially photoselected, which suggests an ultrafast interligand randomization of the MLCT state.

1. Introduction

Ruthenium tris bipyridine, $[\text{Ru}(\text{bpy})_3]^{2+}$, is commonly used as a photosensitizer due to its ability to be reversibly reduced and oxidized, its ability to form stable complexes, and the long lifetime of its excited state. The lowest excited state of $[\text{Ru}(\text{bpy})_3]^{2+}$ can be described as a metal to ligand charge transfer (MLCT) state.^{1,2} If the molecule were perfectly symmetric, the excited state would be symmetric and the excess electron would be evenly shared between the three ligands. However, it is known that the relaxed excited state is best described as one formally reduced bpy and two neutral ones.^{1–3} This means that the symmetry is broken by solvent fluctuations or intramolecular vibrations and the excess electron becomes localized. There has been some debate over whether photoexcitation directly causes the electron to localize on one ligand or if the localization is caused by solvent and vibrational trapping.^{1,2} Recently, resonance Raman experiments have strongly suggested that a localized MLCT state is formed already in the excitation process.⁴ In any case, once the electron has localized on one ligand it can “hop” to the other ligands, and this is sometimes denoted “interligand electron transfer”. This interligand electron transfer is of fundamental interest and is important in ruthenium polypyridine based photoactive molecular assemblies. For example when an electron acceptor molecule or semiconductor particle is attached via one of the ligands of the ruthenium complex the overall electron-transfer rate may be limited by the “hopping” of the excited state to the bridging ligand from which the electron transfer can occur.

A way of measuring both the nature of the excited state and the rate with which the localized electron “hops” from one ligand to another is through emission or transient absorption anisotropy measurements. In an anisotropy measurement, the magnitude of the anisotropy gives information of the relative direction of the excited and probed transitions. If the direction of the transition dipole moments for the different states involved are known, conclusions can then be drawn about the nature of the

excited state. This has been done for $[\text{Ru}(\text{bpy})_3]^{2+}$ by several groups. The steady state emission anisotropy in a solvent glass at 77 K gives an initial value close to the expected value for a linear oscillator. The authors attributed the initial value to that for a state with the electron localized on the same ligand as the one that was initially photoselected.⁵

Pump probe transient absorption anisotropy measurements using 30 ps fwhm laser pulses pumping at 460 nm and probing at 355 nm gave a biexponential anisotropy decay with time constants of 12 and 50 ps in room-temperature acetonitrile.⁶ The authors attributed the 12 ps component to electron hopping between ligands. The observed time constant is given by the sum of hopping rates between all ligands as well as rotation and corresponds to a time constant of 47 ps for hopping from one ligand to another.⁶ The 50 ps component was attributed to rotational diffusion. A similar experiment but exciting and probing at 480 nm using 25 fs fwhm laser pulses showed a fast initial anisotropy decay on a 60 fs time scale followed by a constant value up to 1 ps.⁷ The authors assumed that the “final” state at 1 ps is before any hopping had taken place, based on the conclusions in ref 6, and they assumed that no other processes can give anisotropy decay on the observed 60 fs time scale. By exclusion and because of a high initial anisotropy value, they then attribute the 60 fs decay to decoherence since this can also lead to anisotropy decay.⁸

Our group has reported electron transfer from excited $[\text{Ru}(\text{bpy})_3]^{2+}$ to a methyl viologen covalently linked to one of the bipyridines with a time constant of 4 ps.⁹ From electrochemical data, interligand electron transfer from the unsubstituted to the substituted bipyridine was known to be isoenergetic. The initial MLCT state would then be localized on the different bipyridines with equal probability. Consequently, if the hopping time constant was around 47 ps as reported in ref 6, the observed electron transfer to the methyl viologen would have been limited by hopping to the binding ligand in approximately two-thirds of the complexes. Instead we observed a single-exponential reaction with a 4 ps lifetime.⁹ We therefore decided to reinvestigate the hopping dynamics in $[\text{Ru}(\text{bpy})_3]^{2+}$ with ~ 100 fs laser pulses and probing with white light in the range 340–650 nm. To get reference values for the anisotropy in the case

* To whom correspondence should be addressed. E-mail: leif.hammarstrom@fki.uu.se.

[†] Department of Physical Chemistry.

[‡] Department of Chemistry, Organic Chemistry.

when interligand electron hopping is not possible, we have also done the same measurements on $[\text{Ru}(\text{bpy})(\text{py})_4]^{2+}$.

2. Experimental Section

All measurements were done in acetonitrile. $[\text{Ru}(\text{bpy})_3]^{2+}$ was purchased from Molecular Probes, a change of counterion from Cl^- to PF_6^- was done by Dr. Licheng Sun, Stockholm. $[\text{Ru}(\text{bpy})(\text{py})_4](\text{PF}_6)_2$ was prepared as follows: In an argon atmosphere, pyridine (19.2 μL , 237 μmol) was added to a solution of $[\text{Ru}(\text{bpy})(\text{DMSO})_4](\text{PF}_6)_2$ ^{10,11} (123 mg, 47.4 μmol) in ethanol (5 mL, 99.7%). The solution was heated to 80 °C for 19 h. The dark red-brown solution was allowed to cool to room temperature before NH_4PF_6 (155 mg, 948 μmol) was added. The mixture was stirred at -26 °C for 3 h before the formed precipitate was filtered off and washed with water. Drying in vacuo yielded 13 mg of the desired complex (32%). The product was not stable. ¹H NMR (acetone-*d*₆) δ (ppm) 10.03, 9.10, 8.58, 8.42, 8.28, 8.10, 8.05, 8.04, 7.68–7.79, 7.50, 7.12–7.21

Femtosecond transient absorption measurements were made using an amplified 1 kHz Ti:sapphire laser system. An optical parametric amplifier (TOPAS) was used to produce 480 nm, 100 fs excitation pulses. The pump passed a chopper in which every other pulse was blocked before it was focused in the sample cell (0.2 or 1 mm quartz cuvette). The sample cell was mounted on a holder which moved up and down with a frequency of about 1 Hz. The probe beam was led through a delay line and focused on a CaF_2 plate where a white light continuum (WL) was generated. A beam splitter was used to produce a WL reference beam. The probe and reference were focused through the slit of a monochromator and detected by two 512 pixel diode arrays of a detector system constructed by Dr. Torbjörn Pascher, Lund. Transient absorption spectra are the average of 10 scans with 1000 shots at each time step. The absorbance of the sample was about 0.3 at the excitation wavelength. By convoluting the signal with a Gaussian pulse, the instrument response function was estimated to 150 fs above 400 nm, 300 fs at 360 nm in a 1 mm cuvette and 200 fs in a 0.2 mm cuvette. The response function measured as the fwhm of the signal from pure solvent gives similar values. Experiments with pump pulses of both 0.8 and 1.6 μJ were compared and showed no significant difference. The experiments shown in the article are with 1.6 μJ pump pulses and 1 mm cuvettes.

3. Results

3.1. Absorption Spectra and Choice of Excitation Wavelength. Absorption spectra for $[\text{Ru}(\text{bpy})_3]^{2+}$ and $[\text{Ru}(\text{bpy})(\text{py})_4]^{2+}$ are given in Figure 1. Our spectra correspond fairly well to earlier published spectra on the same complexes.^{1,12} The band around 285 nm in both complexes is a ligand centered (LC) π to π^* transition on the bipyridine; the transition around 360 nm for $[\text{Ru}(\text{bpy})(\text{py})_4]^{2+}$ is metal to ligand charge transfer (MLCT) involving the pyridine; and the transitions around 450 nm for $[\text{Ru}(\text{bpy})_3]^{2+}$ and around 500 nm for $[\text{Ru}(\text{bpy})(\text{py})_4]^{2+}$ are MLCT transitions involving the bipyridine.^{1,12}

To minimize effects from vibrational and solvent relaxation, to get a pure excitation of the lowest MLCT transition, and to simplify comparison with previous work,^{7,13} we have excited at 480 nm which is at the red edge of the metal to bipyridine absorption band at 480 nm of $[\text{Ru}(\text{bpy})_3]^{2+}$. We have then probed all wavelengths between 350 and 640 nm using white light, but we will focus on the dynamics at 360, 450, and 610 nm. At 360 nm, mainly the excited-state absorption of the reduced bipyridine is probed,^{1,14} at 450 nm, mainly ground-

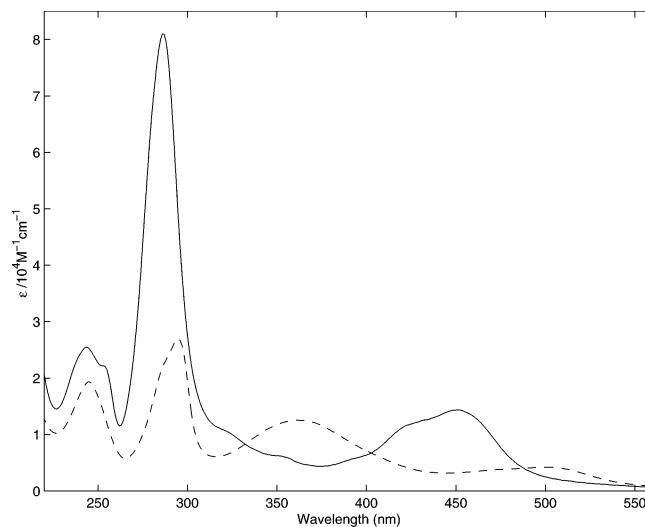


Figure 1. Ground-state absorption of $[\text{Ru}(\text{bpy})_3]^{2+}$ (full line) and $[\text{Ru}(\text{bpy})(\text{py})_4]^{2+}$ (dashed line).

state bleach is probed, and at 610 nm, the pure excited-state absorption is probed.

3.2. Transient Absorption at Magic Angle. Magic angle signals have been constructed by adding the signal from parallel pump and probe and twice the signal from perpendicular pump and probe. The main features of the spectra are formed within the time resolution of our experiment. The magic angle transient absorption spectra for $[\text{Ru}(\text{bpy})_3]^{2+}$ is given in Figure 2A and for $[\text{Ru}(\text{bpy})(\text{py})_4]^{2+}$ in Figure 2B. The spectra for $[\text{Ru}(\text{bpy})_3]^{2+}$ correspond well to earlier published spectra on a nanosecond time scale.¹⁴ They also agree with femtosecond pump probe spectra, which were limited to the range 440–530 nm.¹³ We are not aware of any published transient absorption spectra for excited $[\text{Ru}(\text{bpy})_3]^{2+}$ on this time scale that extend below 400 nm, resolving the transient 360 nm band. Also there are to our knowledge no published excited-state spectra of $[\text{Ru}(\text{bpy})(\text{py})_4]^{2+}$. Both complexes have excited state transitions around 360 nm with roughly the same shape, the band is very similar to the ground-state absorption of reduced bipyridine,^{15,16} and is therefore assigned to transitions of a reduced bipyridine.^{1,2,6} The band around 360 nm looks similar in both complexes and is dominated by excited-state absorption. Around 450 nm, the signal in both complexes is dominated by ground-state bleach. At higher wavelengths there is again positive transient absorption as there is no significant ground-state absorption above 550 nm. For excited $[\text{Ru}(\text{bpy})_3]^{2+}$, absorption above 400 nm is attributed to a combination of transitions from the unreduced bipyridines to the formally oxidized ruthenium, LMCT, and lower energy transitions on the reduced bipyridine.¹ Corresponding transitions will also be present in the spectrum for excited $[\text{Ru}(\text{bpy})(\text{py})_4]^{2+}$. The LMCT transition from pyridine to Ru^{III} will be blue shifted due to the higher reduction potential of pyridine which makes it reasonable to assign the peak around 400 nm to these and the absorption at higher wavelengths to be only transitions on the reduced bipyridine. For $[\text{Ru}(\text{bpy})_3]^{2+}$, we observe some early time dynamics that give rise to small transient absorption changes at magic angle, most notably a rise of the band around 360 nm with a fast component around 0.3 ps and a slow, 5–15 ps, component, see Figure 3. No signal changes were observed at longer times (up to 1 ns) consistent with the ca. 100 ns excited-state lifetime of $[\text{Ru}(\text{bpy})_3]^{2+}$ in aerated acetonitrile. On a subpicosecond time scale, the same qualitative results can be observed in $[\text{Ru}(\text{bpy})(\text{py})_4]^{2+}$ (Figure 4) although the subpicosecond rise around 360 nm is more pronounced and somewhat

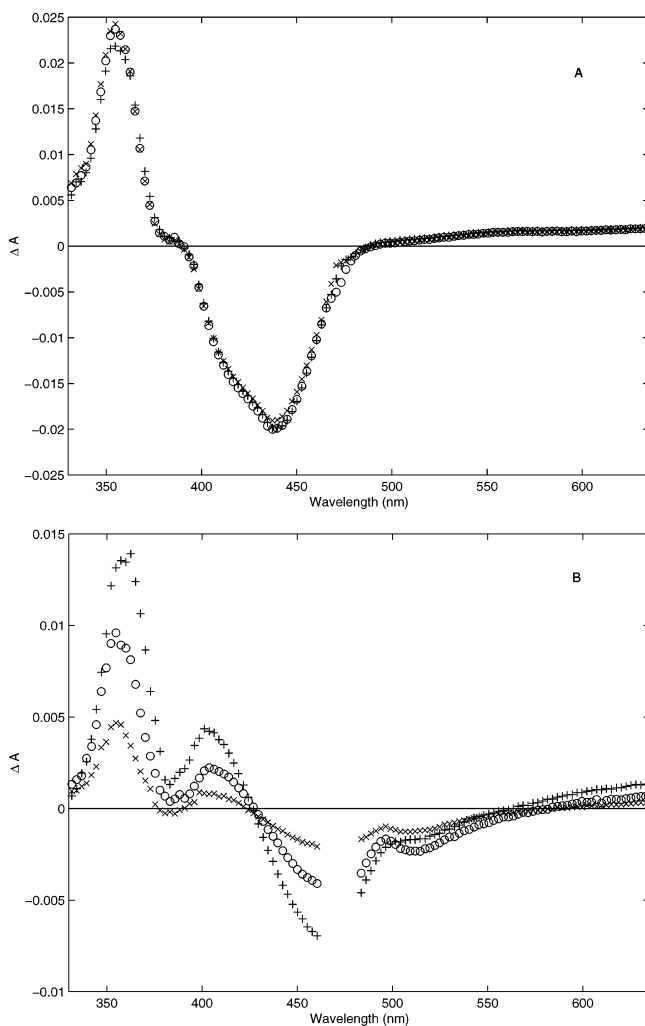


Figure 2. (A) Transient absorption spectra of $[\text{Ru}(\text{bpy})_3]^{2+}$ at 1 ps (plus signs), 100 ps (circles), and 1 ns (crosses). (B) Transient absorption spectra of $[\text{Ru}(\text{bpy})(\text{py})_4]^{2+}$ at 1 ps (plus signs), 100 ps (circles), and 1 ns (crosses). $\lambda_{\text{ex}} = 480$ nm, solvent: acetonitrile.

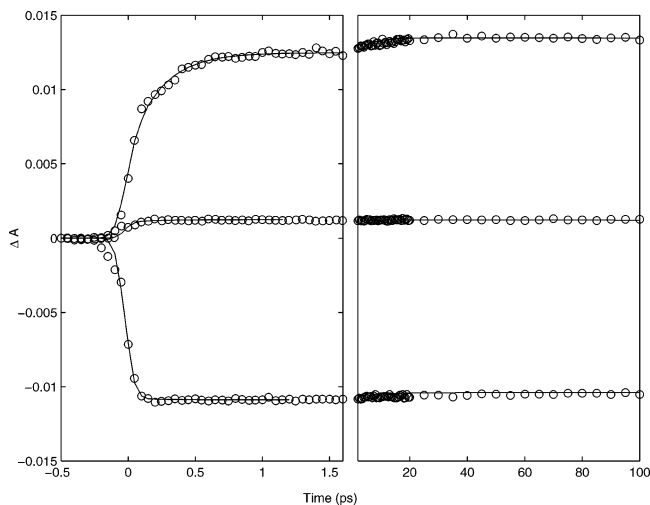


Figure 3. Magic angle signal and biexponential fit convoluted with response function of $[\text{Ru}(\text{bpy})_3]^{2+}$ at 360 (upper curve), 450 (lower curve), and 610 nm (middle curve).

slower (0.8 ps). At longer times, $[\text{Ru}(\text{bpy})(\text{py})_4]^{2+}$ instead shows a triexponential decay to the ground state with time constants around 20 ps (25% of total signal), 100 ps (15%), and 1.3 ns (60%).

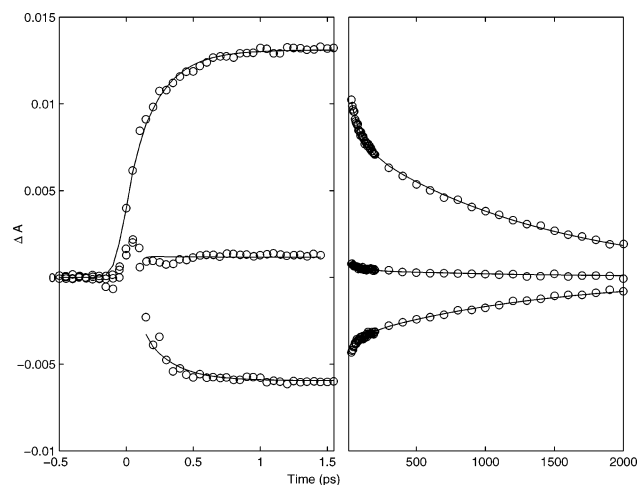


Figure 4. Left half: Magic angle signal and biexponential fit convoluted with response function of $[\text{Ru}(\text{bpy})(\text{py})_4]^{2+}$ for the first 2 ps at 360 (upper curve), 450 (lower curve), and 610 nm (middle curve). Right half: Data at later times and a triexponential fit started at 5 ps.

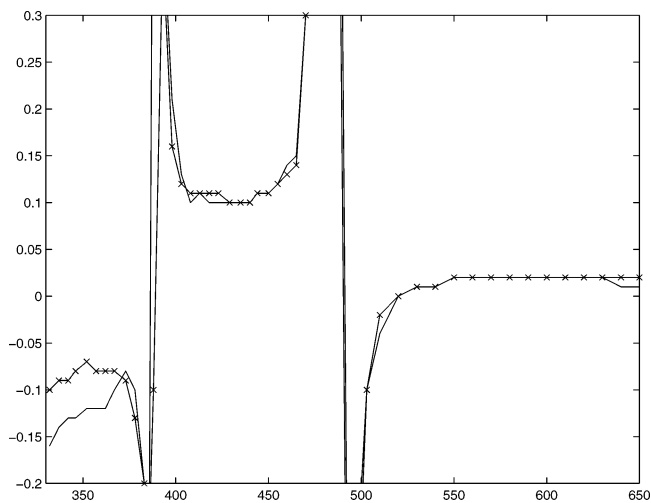


Figure 5. Measured anisotropy spectra for $[\text{Ru}(\text{bpy})_3]^{2+}$ 100 fs after excitation, full line, and after 1 ps, crossed line.

3.3. Transient Absorption Anisotropy. Time and wavelength resolved anisotropy values were constructed from the signal with parallel pump and probe minus the signal with perpendicular pump and probe divided by the magic angle signal. The transient absorption anisotropy for $[\text{Ru}(\text{bpy})_3]^{2+}$ versus wavelength is shown in Figure 5. To fit the anisotropy decays at the three selected wavelengths, 360, 450, and 610 nm, simultaneously, three exponentials were needed for both complexes (Figures 6 and 7). The slowest component, 50 ps for $[\text{Ru}(\text{bpy})_3]^{2+}$ and 40 ps for $[\text{Ru}(\text{bpy})(\text{py})_4]^{2+}$, correspond well to earlier measurements⁶ where it was attributed to rotational diffusion of the complex. A small component decaying on a picosecond time scale, around 5 ps for $[\text{Ru}(\text{bpy})_3]^{2+}$ and 16 ps for $[\text{Ru}(\text{bpy})(\text{py})_4]^{2+}$, is present both at 360 and 450 nm. Finally, there is a subpicosecond component mainly visible at 360 nm for $[\text{Ru}(\text{bpy})_3]^{2+}$ and at 360 and 450 nm for $[\text{Ru}(\text{bpy})(\text{py})_4]^{2+}$. Fits are shown in Figures 6 and 7, and the resulting lifetimes and amplitudes are given in Table 1. The amplitudes of the 16 and 40 ps components for $[\text{Ru}(\text{bpy})(\text{py})_4]^{2+}$ vary with the initial guesses in the fitting process but the sum of the two amplitudes does not. The measured anisotropy for $[\text{Ru}(\text{bpy})_3]^{2+}$ at 360 nm after five picoseconds is -0.08 , a value which matches well the initial anisotropy measured in ref 6. The value at 480 nm after 1 picosecond is 0.40 which matches well the

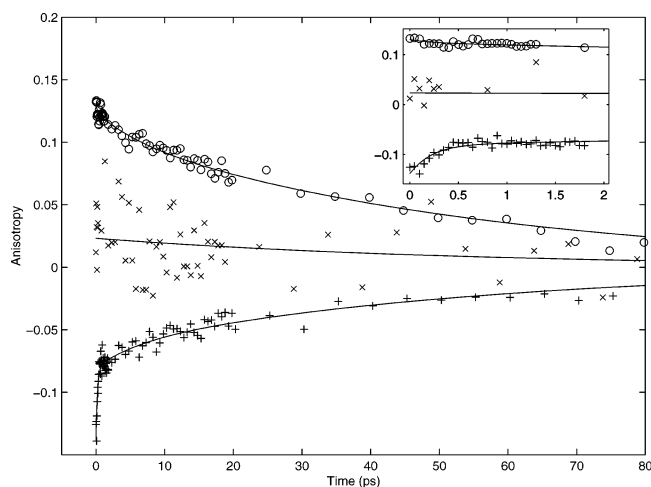


Figure 6. Global fit of anisotropy decay for $[\text{Ru}(\text{bpy})_3]^{2+}$ at 360 (plus signs), 450 (circles), and 610 (crosses) nm. Inset shows the first two picoseconds.

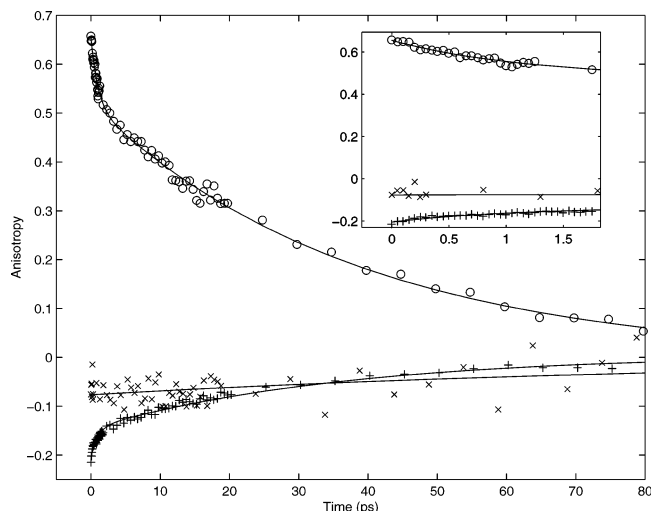


Figure 7. Global fit of anisotropy decay for $[\text{Ru}(\text{bpy})(\text{py})_4]^{2+}$ at 360 (plus signs), 450 (circles), and 610 (crosses) nm. Inset shows the first two picoseconds.

anisotropy after 1 ps at 480 nm measured in ref 7. Our measured kinetics are somewhat different from those measured in ref 6, which is probably due to the limited time resolution, 30 ps, in their experiment. Also we obtained transient absorption magic angle and anisotropy data in the whole spectral region 340–650 nm, on a subpicosecond time scale which allowed us to draw new conclusions.

4. Discussion

4.1. Magic Angle Dynamics. From 50 ps to 1 ns, $[\text{Ru}(\text{bpy})_3]^{2+}$ exhibits no dynamics, as could be expected since the lifetime in acetonitrile with air present is around 100 ns. The multiexponential decay in $[\text{Ru}(\text{bpy})(\text{py})_4]^{2+}$ is probably due to the fact that the pyridines readily are substituted. One or several pyridines can be replaced by solvent or counterion either as an effect of excitation or already before the experiment. Fortunately, because bipyridines are generally strongly coordinating, and because the transient absorption peak corresponding to reduced bipyridine is present at all times, we can safely assume that the bipyridine is coordinated at all times. The yield of pyridine loss is small, as the ground state absorption spectrum shows a decrease of the metal-to-pyridine band only after extensive measurements, and the metal-to-bipyridine band is not decreased

TABLE 1: Results of Global Fits of Anisotropy Decay for $[\text{Ru}(\text{bpy})_3]^{2+}$ and $[\text{Ru}(\text{bpy})(\text{py})_4]^{2+}$

	lifetime τ , (ps)	anisotropy amplitude		
		360 nm	450 nm	610 nm
$[\text{Ru}(\text{bpy})_3]^{2+}$	0.3	-0.05	0.02	
	5	-0.02	0.01	
	50	-0.06	0.11	0.03 ^a
$[\text{Ru}(\text{bpy})(\text{py})_4]^{2+}$	0.8	-0.06	0.13	
	16	-0.06	0.05	
	40	-0.10	0.48	-0.06 ^a

^a A single exponential was used at 610 nm since the low signal-to-noise ratio did not allow for resolution of faster components.

but somewhat blue shifted. Since pyridines, substituted solvent ligands, and counterions all are much worse electron acceptors than bipyridine, we can treat the molecule as a ruthenium with only one active bipyridine ligand, on which the lowest MLCT state is localized, and the others as spectator ligands.² This gives the desired reference complex for the anisotropy measurements where interligand electron hopping will not be observed.

The observed 0.3 and ~ 10 ps isotropic dynamics at 360 nm seems to be in conflict with the results in ref 13 where the authors see no isotropic dynamics after the first 300 fs. The apparent discrepancy is probably due to the fact that they probe at 400–500 nm where ground state bleach is dominating, whereas the 360 nm feature is an excited state absorption from the formally reduced bipyridine. This is where most of the solvation and vibrational relaxation can be expected to occur, and this transition should be the most sensitive probe of these processes. Indeed the only wavelength where we observe any significant ~ 10 ps isotropic dynamics is around 360 nm. Around this wavelength, similar picosecond dynamics have been observed in $[\text{Re}(\text{Etpy})(\text{CO})_3(\text{dmb})]^+$ and $[\text{Re}(\text{Cl})(\text{CO})_3(\text{bpy})]$ in acetonitrile.¹⁷ Additionally the authors in ref 13 do observe biexponential dynamics ($\tau_1 = 120$ fs, $\tau_2 = 5$ ps) for $[\text{Ru}(\text{bpy})_3]^{2+}$ which they attributed to vibrational cooling when exciting at 400 nm, at the blue edge of the MLCT band.¹⁸ This may be the same relaxation process as the one we observe, but as excitation was performed with larger excess energy, the relaxation amplitude may have been large enough to be observed also in the visible region.

The presence of a subpicosecond component in both $[\text{Ru}(\text{bpy})(\text{py})_4]^{2+}$ and $[\text{Ru}(\text{bpy})_3]^{2+}$ means that we cannot be observing a transition from a state delocalized over all three ligands to a state localized on one, as a delocalized state is impossible in $[\text{Ru}(\text{bpy})(\text{py})_4]^{2+}$.

4.2. Transient Absorption Anisotropy. The measured optical anisotropy depends on the relative direction of the excited and probed dipoles. In the case of $[\text{Ru}(\text{bpy})_3]^{2+}$, this means that we can distinguish between two limiting cases: (i) the bipyridine which was initially photoselected is the one that is formally reduced, and we will denote this the nonrandomized case since the molecule still remembers how it was excited; (ii) all bipyridines have equal probability of being formally reduced irrespective of their orientation relative to the exciting light, and we will denote this the randomized case since the molecule has lost all memory of how it was excited. The randomized case can be reached by interligand hopping in the relaxed MLCT state, but also in the nonrelaxed state at very early times. We will use our anisotropy data to determine the time scale of randomization.

In a pump probe anisotropy experiment, the situation is complicated by the fact that the signal is a sum of three different contributions: excited-state absorption, ground-state bleach, and

stimulated emission. Stimulated emission will make no contribution at 360 and 450 nm. At 610 nm, it could contribute on a subpicosecond time scale,¹⁹ but since we only consider picosecond dynamics at 610 nm, it will not be further discussed. The presence of several anisotropic contributions means that a change of the relative amplitudes of the bleach and excited state absorption components of the signal can change the anisotropy. Thus, a change in the isotropic signal may result in a change in anisotropy. A more detailed discussion on expected anisotropy values and the assumptions we have used to calculate them is given in the appendix, but we will give a brief summary here of which transitions are involved at our chosen wavelengths. Note that there is a residual anisotropy also in the randomized case that is lost only by rotational diffusion of the complex.

At 610 nm, neither of the complexes has any ground-state absorption. Ground-state absorption around 450 nm will be due to MLCT transitions for both complexes. These transitions are directed from the Ruthenium to the center of one of the bipyridines.²⁰ The nature of the weaker ground-state transitions at 360 nm is more uncertain. $[\text{Ru}(\text{bpy})_3]^{2+}$ has some MLCT, some metal centered (MC), and some ligand centered (LC) character, whereas $[\text{Ru}(\text{bpy})(\text{py})_4]^{2+}$ transitions are mainly MLCT from the ruthenium to the pyridine ligands.^{1,12,21} Fortunately, the absorption of the ground state is much smaller than that of the excited state at 360 nm (see results). Excited-state transitions on the reduced bipyridine, giving rise to the band at 360 nm and a part of the transitions at 450 and 610 nm, are directed along the long axis of the reduced bpy.²² Finally, the LMCT transitions will contribute above 500 nm and are directed from a nonreduced bipyridine to the ruthenium.

As can be seen in Figure 5, the measured pump probe anisotropy goes to very high negative and positive values at the isosbestic points. This is expected since the denominator in the expression for anisotropy, the magic angle signal, goes to zero while the numerator does not. Close to isosbestic points, the anisotropy can have very high values as, e.g., seen at 480 nm by us and in ref 7. For both molecules, the anisotropy goes from minus infinity to plus infinity when going from a positive to a negative magic angle signal at both isosbestic points (390 and 490 nm for $[\text{Ru}(\text{bpy})_3]^{2+}$). This means that at least around these wavelengths the bleach anisotropy is more positive than that of the excited-state anisotropy (see the Appendix). This is to be expected since here the bleach anisotropy is around 0.1, whereas excited-state absorption anisotropy is around zero or negative for both wavelengths and regardless of randomization.

For the excited state localization discussion, we have focused on three wavelengths, 360, 450, and 610 nm, since at these wavelengths the transient absorption signal is dominated by either ground state bleach or transient absorption which simplifies the analysis. This is shown by the fact that the anisotropy values are relatively constant in a wavelength interval around those wavelengths (Figure 5). A comparison between measured anisotropy values at one picosecond after excitation and predicted values for the randomized and nonrandomized cases at these wavelengths is shown in Table 2. At 360 and 450 nm, we also give values from extrapolating the fit to time zero. The measured values for $[\text{Ru}(\text{bpy})_3]^{2+}$ agree with the values expected for a randomized excitation. In contrast, the agreement with the values for a nonrandomized excitation is not good, neither at $t = 1$ ps nor at $t = 0$ ps. For $[\text{Ru}(\text{bpy})(\text{py})_4]^{2+}$, the measured values agree fairly well instead with the expected values for a nonrandomized excitation. Most importantly the measured initial anisotropy for $[\text{Ru}(\text{bpy})_3]^{2+}$ is a lot smaller at 360 and 450 nm

TABLE 2: Measured Anisotropy Values at $\Delta t = 1$ ps and Expected Anisotropy Values for Randomized and Nonrandomized $[\text{Ru}(\text{bpy})_3]^{2+}$ and $[\text{Ru}(\text{bpy})(\text{py})_4]^{2+}$ ^a

	360 nm $\Delta t = 0$	360 nm $\Delta t = 1$ ps	450 nm $\Delta t = 0$	450 nm $\Delta t = 1$ ps	610 nm $\Delta t = 1$ ps
$[\text{Ru}(\text{bpy})_3]^{2+}$					
exp	-0.13	-0.08	0.14	0.12	0.03
rand	-0.14	-0.14	0.13	0.13	0.0
non rand	-0.26	-0.26	0.20	0.20	-0.13
$[\text{Ru}(\text{bpy})(\text{py})_4]^{2+}$					
exp	-0.21	-0.16	0.66	0.53	-0.06
non rand ^b	-0.24	-0.24	0.66	0.66	-0.13
non rand ^c	-0.35	-0.35	0.66	0.66	-0.13

^a At 360 and 450 nm anisotropy values extrapolated to zero are also shown. ^b Lower limit for bleach contribution to signal at 360 nm. ^c Upper limit for bleach contribution to signal at 360 nm.

compared both to the reference $[\text{Ru}(\text{bpy})(\text{py})_4]^{2+}$ and what would be expected for nonrandomized $[\text{Ru}(\text{bpy})_3]^{2+}$. Thus, the results clearly suggest that the lowest ³MLCT state of $[\text{Ru}(\text{bpy})_3]^{2+}$ is randomized on all three ligands at least after 1 ps. The measured values at 610 nm match less well with expected values, presumably due to uncertainties in the relative contribution of LC and LMCT transitions at this wavelength (see the Appendix). Nevertheless, the expected values for nonrandomized $[\text{Ru}(\text{bpy})_3]^{2+}$ and $[\text{Ru}(\text{bpy})(\text{py})_4]^{2+}$, as well as the measured values for $[\text{Ru}(\text{bpy})(\text{py})_4]^{2+}$, are negative, whereas the expected value for randomized $[\text{Ru}(\text{bpy})_3]^{2+}$ is zero and the measured value for $[\text{Ru}(\text{bpy})_3]^{2+}$ is somewhat positive. This further supports the notion that we are probing a randomized state in $[\text{Ru}(\text{bpy})_3]^{2+}$ already after less than a picosecond. Our assigned anisotropy values for the randomized case also match measurements on $[\text{Os}(\text{bpy})_3]^{2+}$ in acetonitrile. This complex shows an initial anisotropy at 370 nm of -0.15 which decays with a time constant of 2.7 ps to -0.10 .²³ The authors assign the -0.10 value to a state where the electron has randomized over the ligands and the 2.7 ps time constant to interligand hopping.

What are then the observed dynamics? The slow, 40–50 ps, decay component matches earlier measurements⁶ well and what could be expected for rotational anisotropy decay. In this process, the remaining anisotropy in the randomized state (or nonrandomized for $[\text{Ru}(\text{bpy})(\text{py})_4]^{2+}$) is lost. The fast and medium components can have several explanations. The time constant of the subpicosecond component of the anisotropy decay is the same as that observed for the magic angle dynamics ($\tau = 300$ fs for $[\text{Ru}(\text{bpy})_3]^{2+}$ and $\tau = 800$ fs for $[\text{Ru}(\text{bpy})(\text{py})_4]^{2+}$). As has been suggested previously for $[\text{Ru}(\text{bpy})_3]^{2+}$,^{5,9} this can most likely be attributed to a combination of vibrational and solvent relaxation and singlet–triplet conversion. The change of the magic angle signal will itself affect the anisotropy, as it changes the excited-state absorption contribution. The magnitude of the magic angle changes is not sufficient to explain all of the anisotropy loss, however, which suggests that also the direction of the transition dipole moment of the excited-state absorption may change. This could be due to vibronic coupling to higher states that changes as vibrational and spin relaxation occurs or a change from partial to full charge transfer on the bipyridine. Also the small-amplitude ca. 5 ps component (ca. 16 ps for $[\text{Ru}(\text{bpy})(\text{py})_4]^{2+}$) can be attributed to a corresponding magic angle dynamic component. We cannot exclude that some of the 300 fs component of the anisotropy decay is due to a randomization of the excited state by inter-ligand electron transfer. Nevertheless, the facts that the time scale is identical to that of the magic angle dynamics, and that a corresponding anisotropy decay was observed for $[\text{Ru}(\text{bpy})(\text{py})_4]^{2+}$ where no randomization can occur, strongly suggest

TABLE 3: Pyridine Coordinates

pyridine nr	X	Y	Z
1	1	0	0
2	-1	0	0
3	0	1	0
4	0	-1	0
5	0	0	1
6	0	0	-1

that the 300 fs component is not associated with randomization. Instead, most of the randomization must occur on a time scale shorter than 300 fs, i.e. in the unrelaxed MLCT state, possibly even in the singlet MLCT state. This is consistent with our anisotropy values at $t = 0$, extrapolated from the fit using the 300 fs time constant (Table 3), which are in agreement with those calculated for a randomized excitation.

Although previous measurements agree with our data, our better time resolution than in ref 6 and broader wavelength range than in ref 7 as well as comparison with the reference complex $[\text{Ru}(\text{bpy})(\text{py})_4]^{2+}$ reveal a more complex anisotropy decay than previously thought. For the hopping discussion,⁶ the complete randomization of the excited state on a subpicosecond time scale means that the subsequent interligand hopping between relaxed states cannot be monitored with pump probe anisotropy as was done on the >10 ps time scale in ref 6. For the ultrafast delocalized to localized transition of the excited state proposed in ref 7, it means that there are several possible explanations to the observed subpicosecond anisotropy decay, and consequently, the measurements in ref 7 cannot safely determine whether the initial excited state of $[\text{Ru}(\text{bpy})_3]^{2+}$ is localized or delocalized. Our data in Figure 5 show how dramatically the anisotropy increases near the isosbestic point around 490 nm which makes it very difficult to predict excited state anisotropy values. This, and not a delocalized state, may possibly explain the high initial values at 480 nm reported in ref 7.

5. Summary

Transient pump probe anisotropy measurements on $[\text{Ru}(\text{bpy})_3]^{2+}$ and $[\text{Ru}(\text{bpy})(\text{py})_4]^{2+}$ with femtosecond time resolution and probing between 340 and 640 nm show that probably already after a few hundred femtoseconds, and definitely after one picosecond, there is no correlation between which bipyridine is initially photoexcited and which bipyridine is formally reduced. Thus, the MLCT excitation is randomized between the ligands already in the unrelaxed state. This may explain why no slow electron-transfer component, limited by interligand electron hopping, was observed in ref 9. The complexes also show multiexponential dynamics in both the isotropic and anisotropic signals indicating that early time dynamics are more complex than previously thought and that simple hopping and decoherence models are not enough to explain the behavior of the complex.

Acknowledgment. The Swedish Foundation for Strategic Research, The Wallenberg Foundation and the Royal Swedish Academy of Sciences are gratefully acknowledged for financial support.

Appendix: Expected Anisotropy Values

The measured anisotropy when exciting one dipole, μ_{ex} and probing another one, μ_{pr} , where μ_i is a unit vector directed along the transition dipole moment is²⁴

$$r = \frac{3[(\vec{\mu}_{\text{ex}})(\vec{\mu}_{\text{pr}})]^2 - 1}{5} \quad (1)$$

Ruthenium tris bipyridine has quasi D_3 symmetry.²⁵ The symmetry is somewhat distorted since the N–Ru–N angle involving only one bipyridine will be smaller than the corresponding angle involving two bipyridines. This will not affect the polarization of MLCT and ligand based transitions since these are directed toward the center of the bipyridines. Using the coordinate system used by Orgel²⁶ and Ferguson²⁷ the D_3 axis is the (111) axis and the pyridines, labeled one to six, will have the coordinates given in Table 3.

Now the pyridines are connected to make bipyridines, see Figure 8. We will denote the bpy formed from pyridines 1 and 4 α , the one from 2 and 5 β , and the one from 3 and 6 γ . MLCT transitions will be directed from the origin to the center of each bipyridine. This gives the following directions for the transition:

$$\vec{\text{MLCT}}_{\alpha} = \frac{1}{\sqrt{2}}(\vec{e}_x - \vec{e}_y) \quad (2)$$

$$\vec{\text{MLCT}}_{\beta} = \frac{1}{\sqrt{2}}(-\vec{e}_x + \vec{e}_z) \quad (3)$$

$$\vec{\text{MLCT}}_{\gamma} = \frac{1}{\sqrt{2}}(\vec{e}_y - \vec{e}_z) \quad (4)$$

Assuming that the ligand centered, LC, transitions are directed along the axis joining two pyridines,^{7,22} they will have the following direction:

$$\vec{\text{LC}}_{\alpha} = \frac{1}{\sqrt{2}}(\vec{e}_x + \vec{e}_y) \quad (5)$$

$$\vec{\text{LC}}_{\beta} = \frac{1}{\sqrt{2}}(\vec{e}_x + \vec{e}_z) \quad (6)$$

$$\vec{\text{LC}}_{\gamma} = \frac{1}{\sqrt{2}}(\vec{e}_y + \vec{e}_z) \quad (7)$$

The anisotropy in a transient absorption measurement is complicated by two facts. First the nature of transitions in the excited state is not always known. Second the measured anisotropy (r) at any wavelength is a combination of contributions from bleach, excited-state absorption and stimulated emission

$$r = \frac{\Delta\text{abs}_{\text{bl}}}{\Delta\text{abs}} r_{\text{bl}} + \frac{\Delta\text{abs}_{\text{ea}}}{\Delta\text{abs}} r_{\text{ea}} + \frac{\Delta\text{abs}_{\text{se}}}{\Delta\text{abs}} r_{\text{se}} \quad (8)$$

In eq 8, Δabs is total transient absorption, whereas $\Delta\text{abs}_{\text{bl}}$, $\Delta\text{abs}_{\text{ea}}$, and $\Delta\text{abs}_{\text{se}}$ are the contributions to the transient absorption from the bleach, excited-state absorption and stimulated emission, respectively. r_{bl} , r_{ea} , and r_{se} are corresponding anisotropies of each component. The contribution from stimulated emission will only be present during the first picosecond,¹⁹ and only above 500 nm, so we will ignore it (it could affect the 610 nm values at early times but these are not part of the analysis). This means that the anisotropy will be strongly dependent on the relative amplitudes of the bleach and excited state absorption component and will go to infinity at isosbestic points. Consequently, changes in the magic angle signal can give rise to changes in the anisotropy even if there is no change in direction of the involved transition dipole moments.

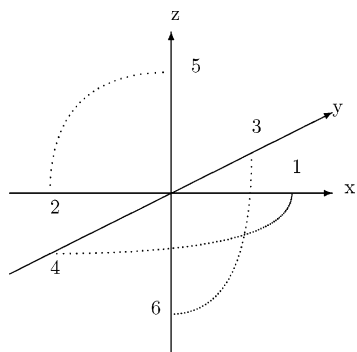


Figure 8. Schematic picture of $[\text{Ru}(\text{bpy})_3]^{2+}$, in which the pyridines are located along the axes (idealized octahedral symmetry).

Excited-state transitions are assumed to be of one of the following types: Transitions along the long axis of the bipyridine perpendicular to the MLCT axis of the same ligand (LC), transitions from an unreduced bipyridine to the metal (LMCT), or in the case of $[\text{Ru}(\text{bpy})(\text{py})_4]^{2+}$ pyridine to metal. Also considered are the cases of a randomized and a nonrandomized excited state where randomized means that all bipyridines have an equal probability of being formally reduced regardless of which one was originally photoselected. These types of transitions give the following expected pump–probe anisotropies for the two studied complexes.

LC Transition, Nonrandomized State. For probing the same bipyridine ligand as the one photoselected in the MLCT excitation

$$r = \frac{3[0.5(\bar{e}_x - \bar{e}_y)(\bar{e}_x + \bar{e}_y)]^2 - 1}{5} = \frac{3 \cdot 0.25 \cdot 0 - 1}{5} = -0.2 \quad (9)$$

and for probing one of the other bipyridine ligands (both give identical results)

$$r = \frac{3[0.5(\bar{e}_x - \bar{e}_y)(\bar{e}_x + \bar{e}_z)]^2 - 1}{5} = \frac{3 \cdot 0.25 \cdot 1 - 1}{5} = -0.05 \quad (10)$$

LC Transition, Randomized State. The resulting anisotropy is the average of the three possibilities

$$r = \frac{1}{3}(-0.2 - 0.05 - 0.05) = -0.1 \quad (11)$$

LMCT Transition, Nonrandomized State. Both bipyridines that are not formally reduced in the excited state give the same result

$$r = \frac{3[0.5(\bar{e}_x - \bar{e}_y)(\bar{e}_x - \bar{e}_z)]^2 - 1}{5} = \frac{3 \cdot 0.25 \cdot 0 - 1}{5} = -0.05 \quad (12)$$

LMCT Transition, Randomized. The result is as for a planar oscillator $r = 0.1$.

LMCT Transitions from Pyridines in Excited $[\text{Ru}(\text{bpy})(\text{py})_4]^{2+}$. All four pyridines give the same result

$$r = \frac{3[0.5(\bar{e}_x - \bar{e}_y)0.5(\bar{e}_x + \bar{e}_z)]^2 - 1}{5} = \frac{3 \cdot 0.25 \cdot 1 - 1}{5} = -0.05 \quad (13)$$

Direction of Transitions in $[\text{Ru}(\text{bpy})_3]^{2+}$. Since all MLCT transitions are bleached regardless of which one was excited, the MLCT bleach at 450 nm will have the anisotropy of a planar oscillator, 0.1. At shorter wavelengths, other transitions will start contributing and lower the anisotropy. Emission anisotropy data exciting at different wavelengths at 77 K suggest a value around 0.05 at 360 nm.²¹ The excited-state absorption at 360 nm is assumed to be 100% LC. Comparing spectra for $\text{Ru}(\text{bpy})_3^{3+}$ and reduced bipyridine gives about two-thirds LMCT character and one-third LC character for the excited-state absorption at 450 nm and 50% of each at 610 nm.¹

Direction of Transitions in $[\text{Ru}(\text{bpy})(\text{py})_4]^{2+}$. The MLCT bleach at 450 nm will have the value of a linear oscillator, 0.4. Unfortunately, there are no polarized emission studies on $[\text{Ru}(\text{bpy})(\text{py})_4]^{2+}$ below 400 nm; however, extrapolating the data in ref 21 indicates a negative anisotropy which corresponds well to the expected value of -0.05 for a metal to pyridine transition, so we will therefore use -0.05 . The excited-state pyridine to ruthenium transitions will be blue shifted compared to the bipyridine to ruthenium transitions in $[\text{Ru}(\text{bpy})_3]^{2+}$. The excited-state absorption at 450 and 610 nm will therefore be assumed to have 50% LC and 50% LMCT character in analogy with $[\text{Ru}(\text{bpy})_3]^{2+}$ at 610 nm. The excited-state absorption at 360 nm is again assumed to be 100% LC because of the high oscillator strength of this transition.

To get expected anisotropy values, we need the relative bleach and excited state absorption contributions as well as the which transitions are involved at the different wavelengths.

Relative Amplitudes for $[\text{Ru}(\text{bpy})_3]^{2+}$ at 360 nm.¹⁴

$$\Delta\text{abs}_{\text{bl}}/\Delta\text{abs}_{\text{ea}} = -0.2 \quad (14)$$

This gives

$$r = \frac{-0.2}{-0.2 + 1}r_{\text{bl}} + \frac{1}{-0.2 + 1}r_{\text{ea}} = -0.25r_{\text{bl}} + 1.25r_{\text{ea}} \quad (15)$$

and at 450 nm

$$\Delta\text{abs}_{\text{bl}}/\Delta\text{abs}_{\text{ea}} = -3$$

This gives

$$r = \frac{-3}{-3 + 1}r_{\text{bl}} + \frac{1}{-3 + 1}r_{\text{ea}} = \frac{3}{2}r_{\text{bl}} - \frac{1}{2}r_{\text{ea}}$$

At 610 nm there is no bleach component so

$$r = r_{\text{ea}}$$

Relative Amplitudes for $[\text{Ru}(\text{bpy})(\text{py})_4]^{2+}$. The fact that the anisotropy values in a wavelength interval around 360 nm are fairly constant suggest a fairly low relative bleach contribution to the signal at 360 nm. This is further supported by the similarity of the 360 nm transient absorption peak in $[\text{Ru}(\text{bpy})_3]^{2+}$ and $[\text{Ru}(\text{bpy})(\text{py})_4]^{2+}$ which suggest a bleach contribution similar to the one in $[\text{Ru}(\text{bpy})_3]^{2+}$, $\Delta\text{abs}_{\text{bl}}/\Delta\text{abs}_{\text{ea}} = -0.2$.

However, the ground-state absorption has an extra peak around 360 nm and the ground-state absorption coefficient at 360 nm is around half the value of the excited-state absorption at the same wavelength, $\Delta\text{abs}_{\text{bl}}/\Delta\text{abs}_{\text{ea}} = -0.5$ see Figure 1, refs 12 and 14. This would give

$$\begin{aligned} r &= \frac{-0.5}{-0.5 + 1}r_{\text{bl}} + \frac{1}{-0.5 + 1}r_{\text{ea}} \\ &= -1r_{\text{bl}} + 2r_{\text{ea}} \end{aligned} \quad (16)$$

The two values will be kept as limiting values. At 450 nm, the same value as for $[\text{Ru}(\text{bpy})_3]^{2+}$ will be used, and at 610 nm, there is again no significant bleach.

This gives the following expected values. $[\text{Ru}(\text{bpy})_3]^{2+}$ Nonrandomized

$$r(360) = -0.25 \cdot 0.05 + 1.25 \cdot (-0.2) \approx -0.26 \quad (17)$$

$$r(450) = 1.5 \cdot 0.1 - 0.5 \cdot \frac{-2 \cdot 0.05 - 0.2}{3} \approx 0.17 \quad (18)$$

$$r(610) = \frac{-0.2 - 0.05}{2} \approx -0.13 \quad (19)$$

$[\text{Ru}(\text{bpy})_3]^{2+}$ Randomized

$$r(360) = -0.25 \cdot 0.05 + 1.25 \cdot -0.1 \approx -0.14 \quad (20)$$

$$r(450) = 1.5 \cdot 0.1 - 0.5 \cdot \frac{2 \cdot 0.1 - 0.1}{3} \approx 0.13 \quad (21)$$

$$r(610) = \frac{-0.1 + 0.1}{2} = 0 \quad (22)$$

$[\text{Ru}(\text{bpy})(\text{py})_4]^{2+}$

$$r(360) = -0.25 \cdot (-0.05) + 1.25 \cdot (-0.2) \approx -0.24 \quad (23)$$

(if the low value for the bleach contribution is used)

$$r(360) = -1 \cdot (-0.05) + 2 \cdot (-0.2) \approx -0.35 \quad (24)$$

(if the high value for the bleach contribution is used) and

$$r(450) = 1.5 \cdot 0.4 - 0.5 \cdot \frac{-0.2 - 0.05}{2} \approx 0.66 \quad (25)$$

$$r(610) = \frac{-0.2 - 0.05}{2} \approx -0.13 \quad (26)$$

Near isosbestic points, the anisotropy can reach extremely high values. The magic angle signal is made up of a excited-state absorption part, $a(\text{es})$, and a bleach of ground-state absorption, $-a(\text{gs})$ $\Delta a = a(\text{es}) - a(\text{gs})$. If the difference in bleach and transient absorption anisotropy is $\Delta r = r_{\text{bl}} - r_{\text{es}}$, the measured anisotropy becomes:

$$\begin{aligned} r &= \frac{a(\text{es})}{\Delta a}r_{\text{es}} + \frac{-a(\text{gs})}{\Delta a}r_{\text{bl}} = \\ &= \frac{a(\text{es})}{\Delta a}r_{\text{es}} + \frac{-a(\text{gs})}{\Delta a}(r_{\text{es}} + \Delta r) = r_{\text{es}} - \frac{a(\text{gs})\Delta r}{\Delta a} \end{aligned}$$

In our case, we observe extremely high positive anisotropy values when Δa is a small negative number and extremely high negative values when Δa is a small positive number. This means that Δr is positive so $r_{\text{bl}} > r_{\text{es}}$.

References and Notes

- (1) Kalyanasundaram, K. *Coord. Chem. Rev.* **1982**, *46*, 159.
- (2) Juris, A.; Balzani, V.; Barigelletti, F.; Belser, P.; Von Zelewsky, A. *Coord. Chem. Rev.* **1988**, *84*, 85.
- (3) Demadis, K.; Hartshorn, C.; Meyer, T. *Chem. Rev.* **2001**, *101*, 2655.
- (4) Webb, A.; Knorr, F.; McHale, J. *J. Raman Spectrosc.* **2001**, *32*, 481.
- (5) Myrick, M.; Blakley, R.; DeArmond, M.; Arthur, M. *J. Am. Chem. Soc.* **1988**, *110*, 1325.
- (6) Malone, R.; Kelley, D. *J. Chem. Phys.* **1991**, *95*, 8970.
- (7) Yeh, A.; Shank, C.; McCusker, J. *Science* **2000**, *289*, 935.
- (8) Wynne, K.; Hochstrasser, R. *Chem. Phys.* **1992**, *171*, 179.
- (9) Lomoth, R.; Häupl, T.; Johansson, O.; Hammarström, L. *Chem. Eur. J.* **2002**, *8*, 102.
- (10) Evans, I.; Spencer, A.; Wilkinson, G. *J. Chem. Soc., Dalton Trans.* **1973**, *2*, 204.
- (11) Zakeeruddin, S.; Nazeeruddin, M. K.; Humphry-Baker, R.; Grätzel, M.; Shklover, V. *Inorg. Chem.* **1998**, *37*, 5251.
- (12) Krause, R. *Inorg. Chim. Acta* **1977**, *22*, 209.
- (13) Damrauer, N.; Cerullo, G.; Yeh, A. Boussie, T.; Shank, C.; McCusker, J. *Science* **1997**, *275*, 54.
- (14) Yoshimura, A.; Hoffman, M.; Sun, H. *J. Photochem. Photobiol. A, Chem.* **1993**, *70*, 29.
- (15) König, E.; Kremer, S. *Chem. Phys. Lett.* **1969**, *5*, 87.
- (16) Hoffman, M.; Simic, M.; Mulazzani, Q.; Emmi, S.; Fuoichi, P.; Venturi, M. *Radiat. Phys. Chem.* **1978**, *12*, 111.
- (17) Liard, D.; Busby, M.; Matousek, P.; Towrie, M.; Vlcek, A. *J. Phys. Chem. A* **2004**, *108*, 2363.
- (18) Damrauer, N.; McCusker, J. *J. Phys. Chem. A* **1999**, *103*, 8440.
- (19) Bhasikuttan, A.; Suzuki, M.; Nakashima, S.; Okada, T. *J. Am. Chem. Soc.* **2002**, *124*, 8398.
- (20) Myrick, M.; Blakley, R.; DeArmond, M. *J. Am. Chem. Soc.* **1987**, *109*, 2841.
- (21) Carlin, C.; DeArmond, M. *Chem. Phys. Lett.* **1982**, *89*, 297.
- (22) Hiratsuka, H.; Sekiguchi, K.; Hatano, Y.; Tanizaki, Y.; Mori, Y. *Can. J. Chem.* **1987**, *65*, 1185.
- (23) Shaw, G.; Brown, C.; Papanikolas, J. *J. Phys. Chem. A* **2002**, *106*, 1483.
- (24) Michl, J.; Thulstrup, E. *Spectroscopy with polarized light*; VCH: New York, 1995.
- (25) Rillema, D.; Jones, S.; Levy, H. *J. C. S. Chem. Commun.* **1979**, *412*, 849.
- (26) Orgel, L. *J. Chem. Soc.* **1961**, 3683.
- (27) Felix, F.; Ferguson, J.; Gudel, H.; Ludi, A. *J. Am. Chem. Soc.* **1980**, *102*(12), 4096.